Electrical Engineering

Active and reactive power conditioning using SMES devices with PMW-CSC: A feedback nonlinear control approach

Walter Gil-González [a,*], Oscar Danilo Montoya [b]

[a] Universidad Tecnológica de Pereira, AA: 97 – Post Code: 660003, Pereira, Colombia
[b] Universidad Tecnológica de Bolívar, Cartagena, Colombia

ABSTRACT

The active and reactive power conditioning using superconducting magnetic energy storage (SMES) systems for low-voltage distribution networks via feedback nonlinear control is proposed in this paper. The SMES system is interconnected to ac grid using a pulsed-width modulated current source converter (PWM-CSC). The dynamical model of the system exhibits a nonlinear structure, which is eliminated by the application of a nonlinear feedback controller based of the expected behavior of the closed-loop system. The steady state analysis under time-domain reference frame to verify the stability properties on the proposed controller is used. The general control rules allow improving different objectives. The robustness and applicability of the proposed controller is tested considering unbalance and harmonic distortion in the voltage provided by the ac grid. It is also considered the possibility to use the SMES system with the proposed controller to compensate the active power oscillations of a wind-generator system.

1. Introduction

Nowadays, energy storage systems (ESS) play an important role to improve the operation of electrical power systems. ESS contribute in power transmission and distribution systems to enhance the operative conditions such as subsynchronous resonance [1,2], power system stability [3,4], load frequency control [5,6] and voltage dynamic regulation in power transmission systems [7]. At the power distribution systems, power oscillations caused by the introduction of distributed generators are reduced, among others [8–11].

The most viable ESS are battery energy storage systems (BESS), flywheel energy storage (FES), pumped hydroelectric storage (PHS), and superconducting magnetic energy storage (SMES) systems [9,10,12,13]. However, BESS, FES, and PHS have some disadvantages compared with SMES systems [14]. In the case of BESS, the efficiency is lower and the service life per load/discharge cycle is shorter than the SMES system [15]. FES systems have a slower response time and need more maintenance than the SMES system. In the case of PHS systems, the limitation comes from the topographic conditions and access to high quality water [16]. The SMES systems have attracted the attention of electric utilities due to their fast response, high-energy storage efficiency (an efficiency around 95%) and, particularly the large amounts of discharge power during small periods of time [9,17,18]. Due to these advantages, SMES systems also have an application, mainly in power distribution systems with high penetration of renewable energy sources (such as wind and solar), where the dynamical performance and electricity supply can be improved [9,15,17].

SMES is a superconducting coil, which is cooled by helium, hydrogen or liquid nitrogen, to reach a temperature close to the absolute zero [10]. This device can store energy in the form of a magnetic field; which is generated by the superconducting coil when a direct current flows through it. In this sense, the magnetic field has stored a constant value of energy; however, when the magnitude of the direct current increases or decreases, the stored energy behaves the same way; which implies that the energy transference can be controlled if the current through the superconducting coil is controlled [9]. Additionally, SMES systems require a power electronic converter to be integrated into the power distribution systems as well as fast and robust control strategies to guarantee their efficient performance [19,20]. There are three types of configurations to integrate SMES systems, depicted in Fig. 1, namely, line commutated converters (LCC) [5,9], voltage source
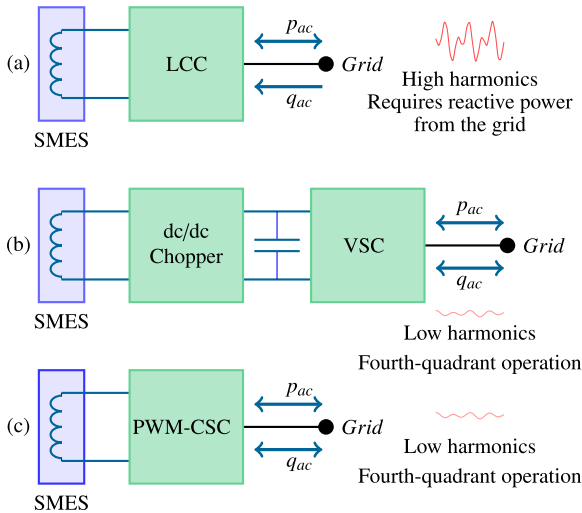
Production and hosting by Elsevier

Fig. 1. Typical interconnection between SMES systems and electrical grid: (a) connection using line commutated converters (LCC), (b) connection using voltage source converters (VSC) and dc/dc converters and (c) connection employing pulse-width-modulated current source converters (PWM-CSC).

converter (VSC) with dc/dc-chopper connection [9,21], and pulse-width modulated current source converter (PWM-CSC) [8,22]. The first type of converter uses thyristors as a switching device. This converter has low switching losses and active power control; however, it has low capacity to control reactive power. In addition, an LCC requires passive filters to mitigate its harmonic injections. The VSC and PWM-CSC permit an independent control of active and reactive power in both directions with low harmonic distortion. In case of VSC, a dc/dc chopper to allow current variations on the superconducting coil is required, while a PWM-CSC allows directly this type of variations. For this reason, it is more natural to use a PWM-CSC to integrate a SMES system into an ac grid than other technologies [9,23,24].

The most classical controller proposed in the specialized literature to operate a power system conditioning using a SMES system is the proportional-integral (PI) strategy [25,26]. Furthermore, this control methodology presents low performance and low robustness, because the SMES system is a non-linear and strongly coupled system [26,27]. To design PI controller Taylor's linearization of some partial linearization is employed, which implies that it is only possible to guarantee stability properties around the operational point [26]. Nevertheless, when there are important deviations concerning the operational point, the PI controller presents low performance and it could have instability [26]. Some authors [28] have proposed an adaptable PI controller by adjusting its parameters via meta-heuristic optimization; notwithstanding, this approach requires more complexity calculations and increases the difficulty of the controller. For the other part, nonlinear control methods such as: fuzzy logic, sliding planes or hysteresis techniques have been proposed to control the SMES system. These techniques of control have shown superior performance when are compared with classical PI methods [29–32]. The fuzzy logic control can be applied to complex systems, enhancing the performance and robustness; but nonetheless, it presents poor steady state performance and its implementation is highly dependent on the control problem. In case of sliding methods, they present a high capacity to reject external perturbations and the possibility to operate with parameter variations; nevertheless, if there are vibration problems in the system, it will reduce the control performance. Finally, in case of hysteresis control, it is easy to implement and has good performance under transient conditions; notwithstanding, the variable frequency of operation makes difficult the filter design.

On the other hand, it is also possible to find strategies such as: linear control by state-feedback [8,33,34], model predictive controllers [35,36] and passivity-based applications [20,37–39], among others. However, there are few non-linear control strategies applied to SMES systems with PWM-CSC, which represents an opportunity for research. In case of CSC there are also control strategies as decoupled state-feedback control [40], classical PI control [23], linear-quadratic regulator control [41], power control theory [42], fuzzy logic control [43], among others.

In this paper, a nonlinear feedback analysis to design a control strategy for a SMES system is proposed based on the expected behavior of the superconducting coil device. It is also presented an analysis of stability under steady-state conditions by using time-domain reference frame via Lyapunov theory. Time domain simulations must demonstrate the soundness and adequate performance of the proposed controller in different cases. These cases contemplate unbalance in voltage, harmonic distortion in voltage and power fluctuations caused by the high variation of weather resources. Additionally, the proposed controller is compared to a conventional PI controller.

The remain of this paper is organized as follows: Section 2 outlines the dynamical model of the SMES. Section 3 the proposed control is explained. Section 4 the simulation scenarios and test system employed are defined. Finally, results are described in Section 5 followed by the conclusions 6 and references list.

2. Dynamical model of SMES with PWM-CSC

Fig. 2 shows the basic configuration of a SMES system with PWM-CSC. The ac side of PWM-CSC is connected to the power grid through a three-phase transformer, and its dc side is directly connected to the superconducting coil [8]. Between the PWM-CSC and the transformer, there is connected a three-phase bank of capacitors to allow the current commutation. Moreover, this bank can filter the high-order harmonics of the ac line current. It is noted that a PWM-CSC is a forced-commutated converter and hence it can control two variables simultaneously [9].

The mathematical model of a SMES system by using a PWM-CSC is obtained through the application of the Kirchoff's laws in the ac side of the converter (see Fig. 2) and applying the power balance between both sides of the converters by employing the Tellegen's theorem. Notice that the mathematical model presented by (1) has been transformed from *abc* reference frame to *dq* reference frame by the application of the Park's transformation considering positive sequence in the ac main grid, it means, by using a classical PLL formulation [44].

$$
\begin{aligned}
L\tfrac{d}{dt}i_d &= v_d - Ri_d - wLi_q - e_d, \\
L\tfrac{d}{dt}i_q &= v_q - Ri_q + wLi_d - e_q, \\
C\tfrac{d}{dt}v_d &= -i_d - wCv_q + m_d i_{dc}, \\
C\tfrac{d}{dt}v_q &= -i_q + wCv_d + m_q i_{dc}, \\
L_{SC}\tfrac{d}{dt}i_{dc} &= -m_d v_d - m_q v_q - R_{SC}i_{dc},
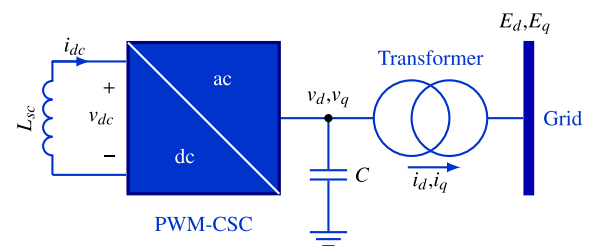\end{aligned}
\tag{1}
$$

Fig. 2. Connection of a SMES system using PWM-CSC.

where i_d and i_q are the direct and quadrature currents (in the dq-frame) of the current flowing to the coupling transformer, L and R are the inductance and resistance of the coupling transformer. The electrical frequency of the ac grid is represented by ω, e_d and e_q are the direct and quadrature voltages of the grid, C is a capacitor used for low-pass filter in the ac side of the PWM-CSC and v_d and v_q are the direct and quadrature voltages at the output of the converter. The m_d and m_q coefficients are the direct and quadrature modulation indices which correspond to the control signals ranged from -1 and 1 (to avoid over-modulation of the power converter). Finally, R_{SC} and L_{sc} correspond to the resistance and inductance of the SMES, is the dc current i_{dc}.

3. SMES control

This section shows the design of a nonlinear control to operate a SMES system connected to the grid by a PWM-CSC. Also, the stability analysis is presented.

The control objective of this paper is to support the active and reactive power from the SMES system to the electrical grid, in order to reduce the power oscillations in the ac grid when renewable energy resources are interconnected. To fulfill this aim, it is necessary to formulate a general control law that allows controlling the ac currents through the transformer. Due to that PWM-CSC does not allow controlling these currents of form direct, it is necessary to make it of form indirect controlling the voltages in the capacitors, this is shown in the next section.

3.1. Controller design

The dynamical formulation of a SMES system with PWM-CSC was presented (1) is composed of five equations. In this set of equations, there are only two control inputs called modulation indices, which are denoted by m_d and m_q. Remark that, the set of Eq. (1) corresponds to an under-actuated system, which implies that there is only one possibility to control two state variables at the same time; nevertheless, it can not control all possible combinations of the state variables since there is a strong relation between them; in this case, i_d and i_{dc}.

To design the controller, the following steps are proposed:

- To control the direct voltage v_d in the bank of capacitor, the third equation of (1) is used to obtain a control law for the direct modulation index m_d, which allows carrying v_d for any arbitrary reference.

$$m_d = i_{dc}^{-1}\left(i_d + \omega C v_q + k_d^v\left(v_d^{ref} - v_d\right)\right), \tag{2}$$

where k_d^v corresponds to a positive proportional gain, that allows controlling the direct voltage.

- To control the quadrature voltage v_q in the bank of capacitor, the fourth equation of (1) is employed to obtain a control law for the quadrature modulation index m_q axis, which enhances to carry v_d for any arbitrary reference.

$$m_q = i_{dc}^{-1}\left(i_q - \omega C v_d + k_q^v\left(v_q^{ref} - v_q\right)\right), \tag{3}$$

where k_q^v corresponds to a positive proportional gain, that enhances to control the quadrature voltage.

- If the objective is to control the direct and quadrature currents i_d and i_q, from the first and second equations of (1) the values of direct and quadrature voltage references v_d^{ref} and v_q^{ref} are obtained, respectively.

$$\begin{aligned}
v_d^{ref} &= R i_d + \omega L i_q + e_d + k_d^i\left(i_d^{ref} - i_d\right), \\
v_q^{ref} &= R i_q - \omega L i_d + e_q + k_q^i\left(i_q^{ref} - i_q\right),
\end{aligned} \tag{4}$$

where k_d^i and k_q^i are the positive proportional gains that enhance to control the direct and quadrature currents, respectively.

- If the objective is to control the current in the superconducting coil, this is, i_{dc}, from the last equation of (1) the value of v_d^{ref} can be obtained, which let on to carry i_{dc} to an arbitrary reference.

$$v_d^{ref} = m_d^{-1}\left(-m_q v_q - R_{SC} i_{dc} - k_{dc}^i\left(i_{dc}^{ref} - i_{dc}\right)\right), \tag{5}$$

where k_{dc}^i is a positive proportional gain that allows controlling the superconducting coil current.

Notice that, there are two possible references for the direct voltage v_d in the terminals of the bank of capacitors. This implies that depending on the control objectives, it is only possible to control the direct current i_d or the superconducting coil current i_{dc} at the same time. This connection between the aforementioned variables is mainly caused by the active power coupling between both sides of the PWM-CSC.

From the other part, it should be noted that the proposed controller corresponds to a nonlinear design based on the dynamic of the system and allows controlling the active and reactive power interchange between the converter and the main grid. To improve this objective, the general expressions that relate the active and reactive power with direct and quadrature currents under the Park's reference frame are [45]:

$$\begin{bmatrix} i_d^{ref} \\ i_q^{ref} \end{bmatrix} = \frac{1}{e_d^2 + e_q^2} \begin{bmatrix} e_d & e_q \\ e_q & -e_d \end{bmatrix} \begin{bmatrix} p_{ac}^{ref} \\ q_{ac}^{ref} \end{bmatrix}. \tag{6}$$

Fig. 3 depicts the proposed controller scheme.

3.2. Closed-loop stable analysis

To guarantee that any state of operation is physically achievable for the SMES system, we can reformulated the dynamical model presented by (1) as follows:

$$\mathcal{P}\dot{x} = [\mathcal{M}(u) - \mathcal{N}]x + \mathcal{E}, \tag{7}$$

where $\mathcal{P}$ is a positive definite matrix, $\mathcal{M}(u)$ is a skew-symmetric matrix that depends on the control inputs $u, \mathcal{N}$ corresponds to a positive semidefinite matrix and $\mathcal{N}$ represents the external non-controllable inputs. These matrices can be obtained by comparison between (1) and (7).

On the aforementioned dynamical system the general concepts about admissible trajectories need to be well-defined in order to develop an efficient control technique that generates on (7) the desired dynamical behavior.

Definition 1. An admissible trajectory $x^\star$ on (7) exists, is differentiable, bounded if and only if it fulfills that:

$$\mathcal{P}\dot{x}^\star = [\mathcal{M}(u^\star) - \mathcal{N}]x^\star + \mathcal{E}, \tag{8}$$

and it is generated by some bounded control input $u^\star$. Finally, an admissible trajectory $x^\star$ is not achieved if does not exist any bounded input that generates it.

Notice that $x^\star$ corresponds in the controller design to the desired operating point which is achieved by the proposed feedback nonlinear approach.

Lemma 1. *The dynamical system (1) in closed-loop operation with the control inputs (2) and (3) and their reference values given in (4) and (5) generates a gradient Hamiltonian system.*

Proof. If the control inputs (2) and (3) and the reference values for the resting of the state variables (4) and (5) are substituting on (1), the following result is achieved:
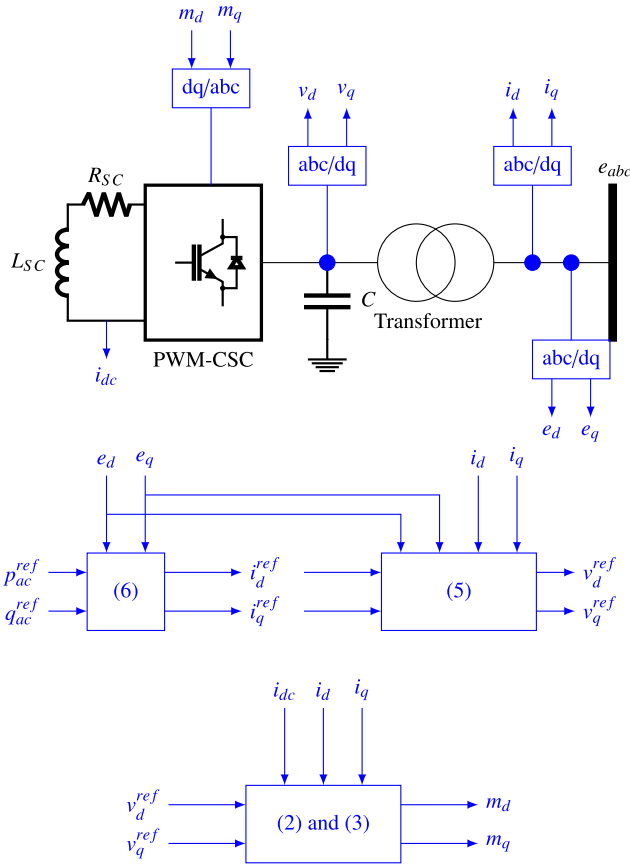
Fig. 3. Proposed controller scheme.

$$L\frac{d}{dt}i_d = k_d^i\left(i_d^{ref} - i_d\right),$$

$$L\frac{d}{dt}i_q = k_q^i\left(i_q^{ref} - i_q\right),$$

$$C\frac{d}{dt}v_d = k_d^v\left(v_d^{ref} - v_d\right), \qquad (9)$$

$$C\frac{d}{dt}v_q = k_q^v\left(v_q^{ref} - v_q\right),$$

$$L_{SC}\frac{d}{dt}i_{dc} = -m_d v_d - m_q v_q - R_{SC}i_{dc},$$

Notice that it is not convenient to replace the control inputs m_d and m_q on the last equation of (9), since a nonlinear relation is generated between the superconducting coil and the rest of state variables. In this sense, we employ for stability purposes an alternative expression for the relationship between the superconducting coil and the ac side variables as follows [8,20]:

$$\frac{1}{2}L_{SC}\frac{d}{dt}i_{dc}^2 = -e_d i_d - e_q i_q - R_{SC}i_{dc}^2. \qquad (10)$$

The superconducting coil behavior depends exclusively of the active power interchange between the SMES system and the main grid [33,38]. Additionally, a new state variable can be defined to replace the quadratic term in (10) as $z = i_{dc}^2, z > 0$, which allows linearizing this expression [19,20].

Now, if we define a new set of variables y, whose minimum is located at the origin of coordinates, generating an equivalent dynamical model presented in (3) and this is a system of Lipschitz:

$$\dot{y} = -\mathcal{K}y + \Gamma, \qquad (11)$$

where

$$\mathcal{K} = \begin{bmatrix} L^{-1}k_d^i & 0 & 0 & 0 & 0 \\ 0 & L^{-1}k_q^i & 0 & 0 & 0 \\ 0 & 0 & C^{-1}k_d^v & 0 & 0 \\ 0 & 0 & 0 & C^{-1}k_q^v & 0 \\ 2L_{SC}^{-1}e_d & 2L_{SC}^{-1}e_d & 0 & 0 & -R_{SC} \end{bmatrix},$$

$$\Gamma = \begin{bmatrix} 0 & 0 & 0 & 0 & -2L_{SC}^{-1}\left(e_d i_d^{ref} + e_q i_q^{ref} - R_{SC}i_{dc}^{ref}\right) \end{bmatrix}^T$$

With the aforementioned definition, the proof is complete.

Proof. Let us consider the following Lyapunov candidate function as:

$$\mathcal{V}(y) = \frac{1}{2}y^T y \qquad (12)$$

with temporal derivative defined as follows:

$$\dot{\mathcal{V}}(y) = -y^T y + y^T \Gamma$$
$$\leqslant -\lambda_{\min}\{\mathcal{K}\}|y|^2 + |y||\Gamma|$$
$$= -(1-\theta)\lambda_{\min}\{\mathcal{K}\}|y|^2 - \theta\lambda_{\min}\{\mathcal{K}\}|y|^2 + |y||\Gamma|$$

with $0 < \theta < 1$, while $\lambda_{\min}\{\mathcal{K}\}$ stands for the minimum eigenvalue of $\mathcal{K}$ and $|\cdot|$ denotes the norm. So, it can be concluded that

$$\dot{\mathcal{V}}(y) \leqslant -(1-\theta)\lambda_{\min}\{\mathcal{K}\}|y|^2 \qquad (13)$$

for all

$$|y| \geqslant \frac{|\Gamma|}{\theta\lambda_{\min}\{\mathcal{K}\}} > 0 \qquad (14)$$

Since $(1-\theta)\lambda_{\min}\{\mathcal{K}\}|y|^2$ is a continuous positive definite function of y, inequality (13) shows that the solutions $y(t)$ are ultimately bounded which concludes the proof [46]. □

4. Test systems and simulation scenarios

4.1. System under study

A SMES connected to an electrical grid through PWM-CSC is shown in Fig. 2 with the parameters given in Tables 1 and 2. Distribution grid configuration is presented in Fig. 4.

Table 1
Parameters values of the microgrid [20].

Parameter	Value	Unit	Parameter	Value	Unit
L_{sis}	2.5	mH	R_{sis}	5	mΩ
L_{12}	1.5	mH	R_{12}	10	mΩ
R_1	1	Ω	R_2	1	Ω
C_1	0.1	μF	C_2	0.1	μF
v_{LL}^{rms}	440	V	–	–	–

Table 2
Parameters values of the SMES system [8].

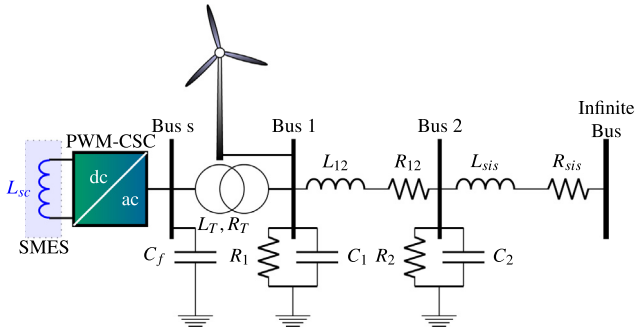| Parameter	Value	Unit	Parameter	Value	Unit
L_T	2.5	mH	R_T	1.25	mΩ
L_{SC}	7.5	H	R_{SC}	0.01	Ω
i_{dc}^{min}	20	A	i_{dc}^{max}	120	A
i_{dc}^{nom}	100	A	Rated dc voltage	375	V
C_f	160	μF	Rated dc voltage	375	V
–	–	–	SMES rating power	37.5	kVA

Fig. 4. Radial distribution network.

4.2. Simulation scenarios

To demonstrate the robustness and effectiveness of the control strategy proposed, we consider the following simulation scenarios:

- First scenario: Showing the capability of the proposed controller to control the superconducting coil current in the SMES.
- Second scenario: Verifying the capability of the proposed controller to support (independently) active and reactive power considering the operating limits of the SMES and voltage unbalance condition in the infinite bus.
- Third scenario: The robustness of the proposed controller considering injection of harmonic distortion in the infinite bus is shown.
- Fourth scenario: Demonstrating the accuracy of the proposed controller for generation with distributed energy resources.

For the first scenario, we consider that the SMES system has been charged previously until its minimal current. For the second and third simulation scenarios, the SMES system has been charged until its nominal current value. Finally, in the fourth scenario, it is considered that the SMES systems is charged up to 90% of its capacity. All the considered scenarios are compared with the classic PI controller. The control gains were tuned with tuning PI controller of Matlab/Simulink. We select the gains of the controllers in such a way that both present an equal dynamic response in order to have fair comparisons. The control gains for both controllers are shown in Tables 3 and 4.

5. Results

The test system was validated in Matlab/Simulink and the SymPowerSystem toolbox, considering a detailed switching model of the semiconductors. The electrical network, PWM-CSC and modulation strategy are presented in Fig. 5. All simulations were

Table 3
The proposed controller gains.

v_d^{ref}	v_q^{ref}	i_d^{ref}	i_q^{ref}
K_d^v	K_q^v	K_d^i	K_q^i
20	20	600	600

Table 4
PI controller gains.

v_d^{ref}		v_q^{ref}		m_d^{ref}		m_q^{ref}	
K_p	K_i	K_p	K_i	K_p	K_i	K_p	K_i
40	10	40	10	400	80	400	80

carried out in a desk-computer INTEL(R) Core(TM) $i5 - 3550, 3.50$ GHz, 8 GB RAM with 64 bits Windows 7 Professional, using MATLAB 2016*a*.

The PWM strategy depicted in Fig. 5 can be studied in [47, ch. 15 sec. 4.1].

5.1. First scenario

In order to demonstrate the tracking capability of the proposed control, the i_{dc}^{ref} current is shown in Fig. 6(a). the term i_{dc} is also depicted in the same plot. In this scenario, v_d^{ref} is presented in (5) which allows controlling the i_{dc} current of direct form.

The proposed control responds appropriately with an error of less than 1%, when the reference is a ramp. Notice that the superconducting coil can be controlled directly by using the direct voltage as intermediate controller as was presented in (5).

In Fig. 6(b) the harmonic distortions for the proposed controller and PI controller are presented. Note that the proposed controller has a Total Harmonic Distortion or THD of 1.73%, being less than the THD in PI controller (THD = 1.96%).

Notice that the THD values are related with the currents flowing through the transformer. The THD is calculated as an average value of the THD present in each electrical-phase.

This strategy of control for the superconducting coil allows controlling the dynamical behavior of the total energy stored in the coil. On the other hand, we do not consider step references for the i_{dc} current, since it implies high power changes in the superconducting coil, which could produce undesired protection operations (see Table 5).

5.2. Second scenario

In this scenario, it is shown the ability of the proposed active and reactive controller, regardless of the SMES. The values for the active and reactive power are arbitrary selected as listed in Table 6. Additionally, it is considered that in the equivalent substation (infinite bus) there is a 10% of unbalance in each phase as follows: $|e_a(t)| = v_{LL}^{rms}, |v_b(t)| = 0.9 v_{LL}^{rms}$ and $|v_c(t)| = 1.1 v_{LL}^{rms}$, respectively.

Notice that the reference values of the active and reactive power are replaced in (6) to obtain the equivalent reference values for the direct and quadrature currents. In this scenario, v_{dq}^{ref} are presented in (4) which permit to control the i_{dq} currents in a direct form.

Fig. 7(a) shows the dynamical response at the dc side of the SMES when this is used to control active and reactive power separately (see Fig. 7(b) and (c)). Also, harmonic contain is shown (see Fig. 7d).

Fig. 7(a) illustrates the behavior of the i_{dc} current which is directly influenced by the active power transferred between ac grid and the power converter, whereas the reactive power characteristic does not affect the current i_{dc}. This implies the possibility to do reactive power compensation without influence the energy storage in the SMES systems due to the reactive power is only produced by the power converter commutation. The only limitation is the current capability of the power converter which must be considered in the tertiary control. Notice that, when p_{ac} is zero, the i_{dc} current keeps constant because there is not power transference between the SMES and ac grid. When p_{ac} is positive, the SMES is bringing energy to the ac grid. That is why it is possible to control energy storage indirectly with active power control.

Fig. 7(b) and (c) show the active and reactive power output in the ac equivalent bus-1. Both controllers respond appropriately, however, the proposed controller has a better performance since it has lower oscillations than PI controller. The active and reactive power oscillates about $\pm 1.18\%$ and $\pm 1.34\%$ respectively, when the
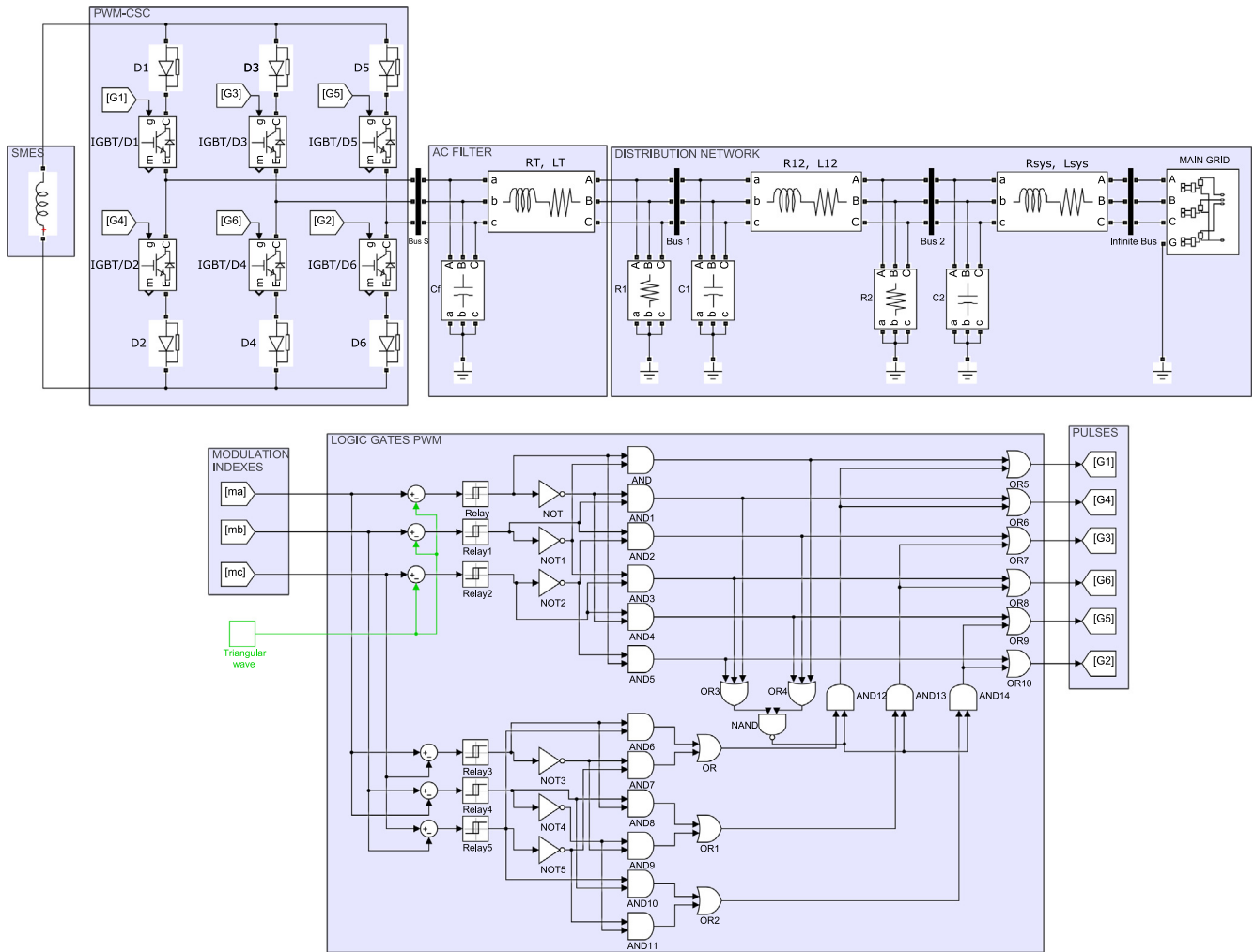
Fig. 5. MATLAB/SIMULINK implementation for test system and PWM strategy.

proposed controller is used. When PI controller is used the oscillations are about ±1.43% for the active power and ±1.78% for the reactive power.

Fig. 7(d) depicts harmonic content both controllers which content a THD of 4.42% and 4.54% for the proposed controller and PI controller, respectively.

5.3. Third scenario

In this scenario, it is shown the robustness of the proposed control to control the active and reactive power regardless the SMES systems. This objective considers a high-magnitude harmonics on voltage signal as given in (15) for the phase *a*. These distortions can be caused by a non-linear load connected to the distribution system. Additionally, the active and reactive power references are the same as those used in the second scenario.

$$v_a(t) = \sqrt{\frac{2}{3}}440 \begin{bmatrix} \cos(\omega t) + \\ \frac{1}{5}\cos\left(5\omega t - \frac{\pi}{6}\right) + \\ \frac{1}{10}\cos\left(7\omega t - \frac{\pi}{3}\right) \end{bmatrix} V \qquad (15)$$

The other phases contemplate the same high magnitude of harmonics considering positive sequence. Fig. 8 shows the response of the SMES system for active and reactive power output in the ac equivalent bus-1, and its content of harmonics.

The active and reactive power delivered-consumed by the SMES system are presented in Fig. 8(a) and (b), respectively. In this sce-

Fig. 6. Superconducting coil current i_{dc} and its harmonic content.

nario the active and reactive power oscillate about ±0.89% and ±1.08% respectively, when the proposed controller is used. In case
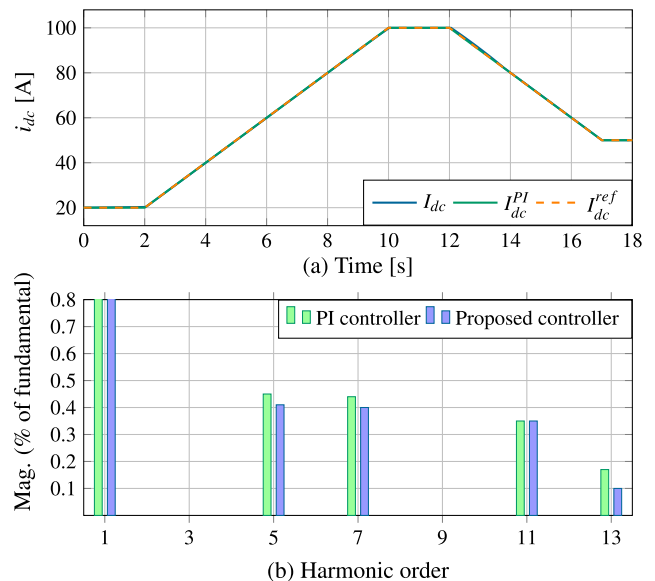
Table 5
Active and reactive power references.

References	Value	t_i [s]	t_f [s]
p_{ac}^{ref} [kW]	0	0	2
	3	2	6
	−2	6	10
	2	10	12
q_{ac}^{ref} [kVAr]	0	0	4
	−4	4	8
	4	8	10
	−2	10	12

Table 6
Active and reactive power references.

p_{ac}^{ref} [kW]	t_i [s]	t_f [s]	q_{ac}^{ref} [kVAr]	t_i [s]	t_f [s]
0	0	2	0	0	4
3	2	6	−4	4	8
−2	6	10	4	8	10
2	10	12	−2	10	12

of the PI controller the oscillations are about ±1.12% and ±1.44% for the active and reactive power, respectively.

Harmonic content for the proposed controller and PI controller is presented in Fig. 8(c). The THD content is of 2.85% for the proposed controller and 3.16% for the PI controller. Note that in this scenario and in the previous case, the proposed controller has a better performance than PI controller.

In scenario of the i_{dc} current there is a similar dynamical behavior as in the second simulation scenario; for this reason its graphic is not presented.

5.4. Fourth scenario

In this scenario, it is presented the possibility to use the SMES systems to support active and reactive power for distributed generation applications. In this scenario, a wind turbine generator type-A (Squirrel-cage Induction Generator-SCIG) connected at the bus-1 (see Fig. 4) which injects the active power and draws the reactive power is considered. Recall that an SCIG turbine requires reactive power from the grid since the induction machine needs magnetization.

For the simulation implementation, the wind generator is dispatched with an active power generation of 2.5 kW. However, the real power is variable and requires to be compensated by the SMES system. Also, at the same time reactive power keeps equal to 0 kVAr. The parameters of the induction generator given in Table 7 were taken from [48]. Fig. 9 shows the active power generated and its consumed reactive power. The main idea to use a SMES system is to reduce the active power oscillations caused by the wind speed variations and support all reactive power required by the induction machine in order to guarantee unity power factor in the bus-1 (see Fig. 4).

The stored energy, active and reactive output power in the bus-1, and its harmonic content are shown in Fig. 10.

Comparing the active power in Fig. 9 with i_{dc} current of SMES in Fig. 10(a), it can be seen that i_{dc} current is increased when the generated power by SCIG is greater than the dispatched power and it decreased otherwise.

Fig. 10(b) shows the accuracy of the proposed control to maintain the active power at 2.5 kW without penalizing the grid operator. In this case, the active power has a standard deviation of 0.52% and 0.83% for the proposed controller and PI controller, respectively.
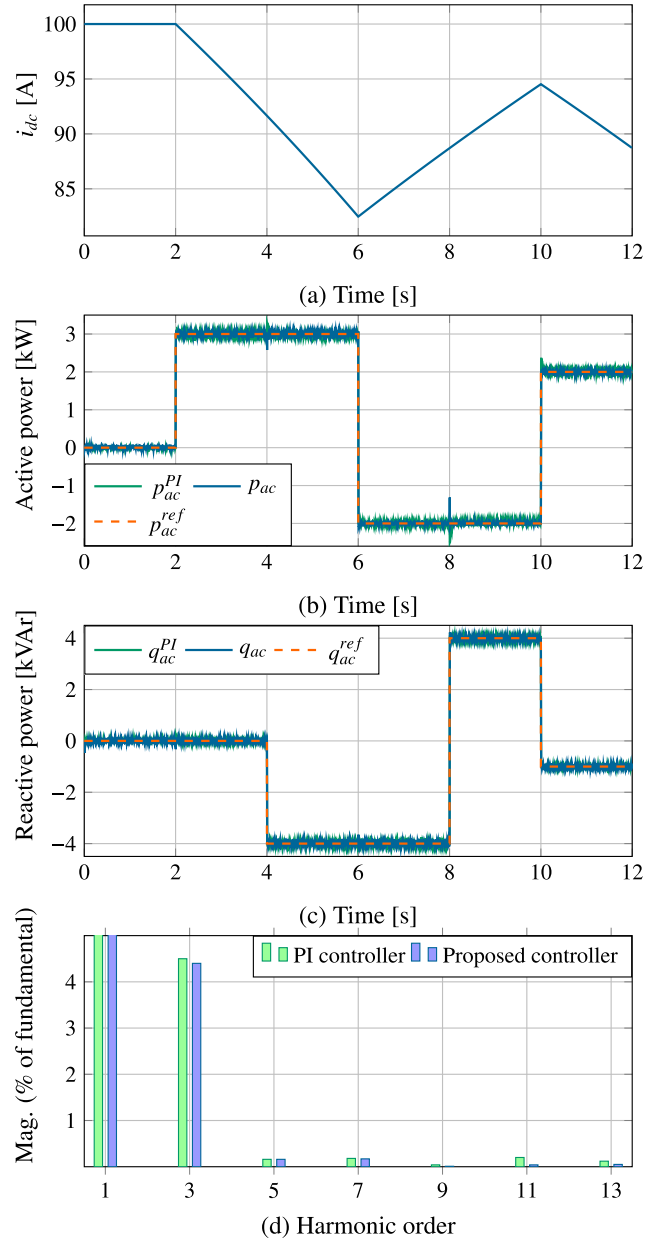

Fig. 7. Dynamical response of active and reactive power control to second scenario for SMES: (a) superconducting coil current i_{dc}, (b) and (c) the active power and reactive power delivered by SMES system p_{ac} and q_{ac}, respectively, and (d) harmonic content.

Recall that the standard deviation corresponds to a statistical measure that allows identifying the variations of a set of arbitrary data around its mean value. In this sense, when are compared the PI controller to the proposed controller considering 2.5 kW as mean value, the PI controller has worst performance than the proposed controller, since the PI controller exhibits strong power oscillations, which is not the case of the proposed controller.

In case of the reactive power, both controllers were maintained at 0 kVAr and thus improving the power factor in bus-1 changing from a power factor of 0.68 ↓ to 1 as shown in Fig. 10(c). Though PI controller presented a better performance.

Fig. 10(d) illustrates the harmonic distortions for support for the active and reactive power. The THD content in this scenario is of 0.82% for the proposed controller and of 0.94% the PI controller.
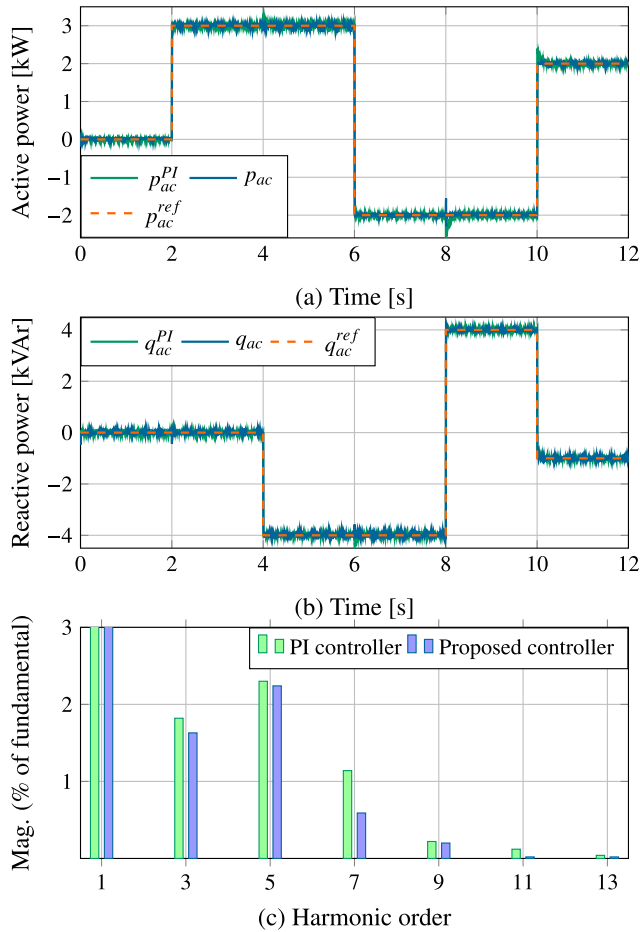
Fig. 8. Dynamical response of active and reactive power control to third scenario for SMES: (a) and (b) the active power and reactive power delivered by SMES system p_{ac} and q_{ac}, respectively, and (c) harmonic content.

Table 7
Induction generator parameters.

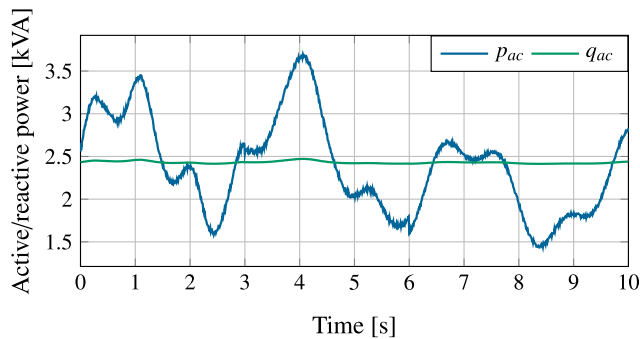| v_{LL}^{rms}	$r_1[\Omega]$	$r_2[\Omega]$	$X_1[\Omega]$	$X_2[\Omega]$	$X_m[\Omega]$
440	0.641	0.332	1.106	0.464	78.9

Fig. 9. Active and reactive power of SCIG.

Note that if a controller contains a lower THD, this has the advantage to have a better waveform quality and has lower losses in VSC, since a part of the losses in the VSC are a function of the THD. Fig. 11 portrays current and voltage of the phase-a in order to show that the proposed controller has a better waveform quality than PI controller.
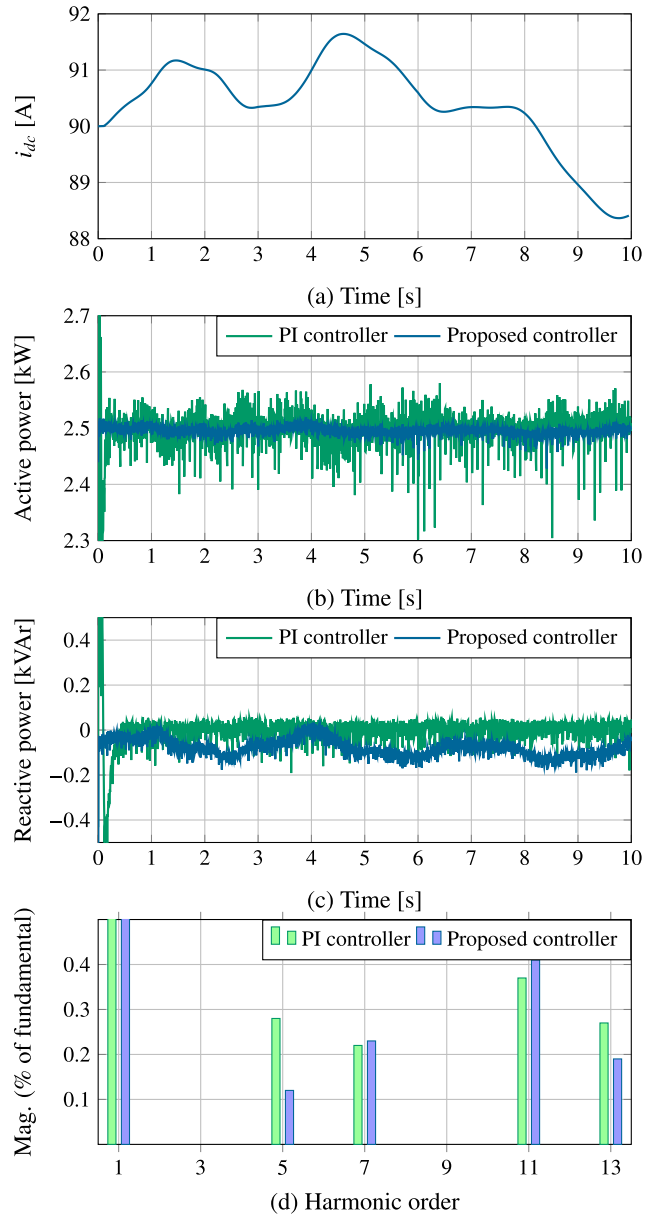

Fig. 10. Dynamical response of active and reactive power control in SMES system to compensate oscillations caused by variations in the speed of wind in the wind generator: (a) superconducting coil current, (b) active power compensation, (c) reactive power compensation, and (d) harmonic content.

6. Conclusion

In this paper, a feedback nonlinear control for SMES system connected to an electric distribution network through a PWM-CSC was presented. This connection was selected because has the advantage to increase the reliability and at the same to reduce the investment costs in electronic devices due to it is not necessary to use a dc/dc chopper in cascade with a voltage source converter. The proposed control strategy showed a good performance to control the active and reactive power of the SMES systems in a wide range of operation, regardless the unbalance and high-harmonic distortion voltage in the ac grid. The proposed control strategy had good robust characteristic and applicability, which could be used to integrate into electric distribution systems, reducing in this way the power fluctuations caused by the high variation of weather as was shown in the fourth scenario. In case of reactive power control capability,
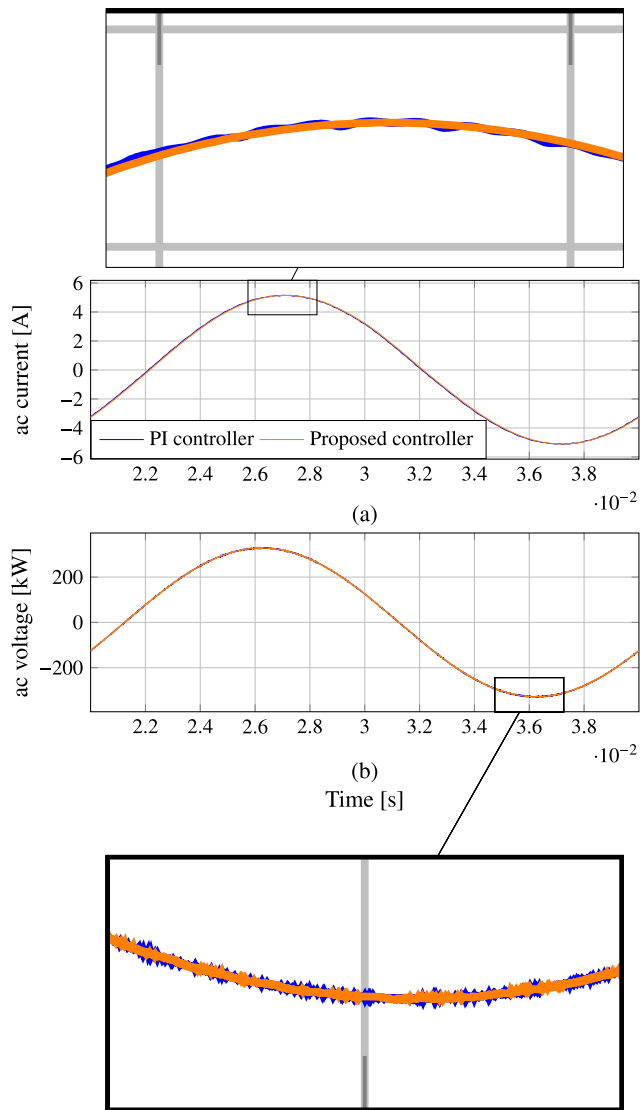
Fig. 11. Waveform of SMES system for fourth scenario: (a) phase-a current and (b) phase-a voltage.

it could be employed to operate as a variable reactor, to improve the power factor of the electrical grids.

7. Financial support

References

[1] Farahani M. A new control strategy of SMES for mitigating subsynchronous oscillations. Physica C 2012;483:34–9.

[2] Gil-González W, Montoya OD, Garces A. Control of a SMES for mitigating subsynchronous oscillations in power systems: a PBC-PI approach. J Energy Storage 2018;20:163–72.

[3] Ortega A, Milano F. Generalized model of VSC-based energy storage systems for transient stability analysis. IEEE Trans Power Syst 2016;31(5):3369–80.

[4] Ali MH, Murata T, Tamura J. Transient stability enhancement by fuzzy logic-controlled SMES considering coordination with optimal reclosing of circuit breakers. IEEE Trans Power Syst 2008;23(2):631–40.

[5] Farahani M, Ganjefar S. Solving LFC problem in an interconnected power system using superconducting magnetic energy storage. Physica C 2013;487:60–6.

[6] Shayeghi H, Jalili A, Shayanfar H. A robust mixed H_2/H_∞ based LFC of a deregulated power system including SMES. Energy Convers Manage 2008;49(10):2656–68.

[7] Huang X, Zhang G, Xiao L. Optimal location of SMES for improving power system voltage stability. IEEE Trans Appl Supercond 2010;20(3):1316–9.

[8] Shi J, Tang Y, Ren L, Li J, Cheng S. Discretization-based decoupled state-feedback control for current Source Power Conditioning System of SMES. IEEE Trans Power Del 2008;23(4):2097–104.

[9] Ali M, Wu B, Dougal R. An overview of SMES applications in power and energy systems. IEEE Trans Sustain Energy 2010;1(1):38–47.

[10] Ibrahim H, Ilinca A, Perron J. Energy storage systems – characteristics and comparisons. Renew Sustain Energy Rev 2008;12(5):1221–50.

[11] Gil-González W, Oscar Danilo Montoya. Passivity-based PI control of a SMES system to support power in electrical grids: a bilinear approach. J Energy Storage 2018;18:459–66.

[12] Montoya OD, Gil-González W, Garces A. SCES integration in power grids: a PBC approach under abc, $\alpha\beta0$ and dq0 reference frames. In: 2018 IEEE PES Transmission & Distribution Conference and Exhibition-Latin America (T&D-LA). IEEE; 2018. p. 1–5.

[13] Montoya OD, Gil-González W, Garcés A, Escobar A, Grisales LF. Nonlinear control for battery energy storage systems in power grids. In: 2018 IEEE Green Technologies Conference; 2018. p. 65–70.

[14] Luo X, Wang J, Dooner M, Clarke J. Overview of current development in electrical energy storage technologies and the application potential in power system operation. Appl Energy 2015;137:511–36.

[15] Ferreira HL, Garde R, Fulli G, Kling W, Lopes JP. Characterisation of electrical energy storage technologies. Energy 2013;53:288–98.

[16] Rehman S, Al-Hadhrami LM, Alam MM. Pumped hydro energy storage system: a technological review. Renew Sustain Energy Rev 2015;44:586–98.

[17] Zakeri B, Syri S. Electrical energy storage systems: a comparative life cycle cost analysis. Renew Sustain Energy Rev 2015;42:569–96.

[18] Montoya O, Gil-González W. Time-domain analysis for current control in single-phase distribution networks using SMES devices with PWM-CSCs. Electr Power Compon Syst 2019:1–10.

[19] Montoya OD, Garcés A, Serra FM. DERs integration in microgrids using VSCs via proportional feedback linearization control: supercapacitors and distributed generators. J Energy Storage 2018;16:250–8.

[20] Montoya OD, Garcés A, Espinosa-Pérez G. A generalized passivity-based control approach for power compensation in distribution systems using electrical energy storage systems. J Energy Storage 2018;16:259–68.

[21] Wang S, Jin J. Design and analysis of a fuzzy logic controlled SMES system. IEEE Trans Appl Supercond 2014;24(5):1–5.

[22] Montoya OD, Gil-González W, Garces A. Control for EESS in three-phase microgrids under time-domain reference frame via PBC theory. IEEE Trans Circ. Syst II: Express Briefs.

[23] Giraldo E, Garcés A. An adaptive control strategy for a wind energy conversion system based on PWM-CSC and PMSG. IEEE Trans Power Syst 2014;29(3):1446–53.

[24] Montoya OD, Gil-González W, Garcés A, Espinosa-Pérez G. Indirect IDA-PBC for active and reactive power support in distribution networks using SMES systems with PWM-CSC. J Energy Storage 2018;17:261–71.

[25] Ortega A, Milano F. Comparison of different control strategies for energy storage devices. In: 2016 Power Systems Computation Conference (PSCC); 2016. p. 1–7.

[26] Liu F, Mei S, Xia D, Ma Y, Jiang X, Lu Q. Experimental evaluation of nonlinear robust control for SMES to improve the transient stability of power systems. IEEE Trans Energy Convers 2004;19(4):774–82.

[27] Tan YL, Wang Y. Stability enhancement using SMES and robust nonlinear control. In: Energy Management and Power Delivery, 1998. Proceedings of EMPD '98. 1998 International Conference on, Vol. 1, 1998, pp. 171–176, vol.1. doi: 10.1109/EMPD.1998.705496.

[28] Vachirasricirikul S, Ngamroo I. Improved H_2/H_∞ control-based robust PI controller design of SMES for suppression of power fluctuation in microgrid. In: 2014 International Electrical Engineering Congress (IEECON); 2014. p. 1–4.

[29] Lu Q, Sun Y, Mei S. Nonlinear control systems and power system dynamics, Vol. 10. Springer Science & Business Media; 2013.

[30] Yi H, Zhuo F, Wang F, Wang Z. A digital hysteresis current controller for three-level neural-point-clamped inverter with mixed-levels and prediction-based sampling. IEEE Trans Power Electron 2016;31(5):3945–57.

[31] Flores-Bahamonde F, Valderrama-Blavi H, Bosque-Moncusi JM, García G, Martínez-Salamero L. Using the sliding-mode control approach for analysis and design of the boost inverter. IET Power Electron 2016;9(8):1625–34.

[32] Tao CW, Wang CM, Chang CW. A design of a dc-ac inverter using a modified ZVS-PWM auxiliary commutation pole and a DSP-based PID-like fuzzy control. IEEE Trans Ind Electron 2016;63(1):397–405.

[33] Gil-González W, Montoya OD, Garcés A, Escobar-Mejía A. Supervisory LMI-based state-feedback control for current source power conditioning of SMES. In: 2017 Ninth Annual IEEE Green Technologies Conference (GreenTech); 2017. p. 145–150.

[34] Gil-González WJ, Garcés A, Escobar A. A generalized model and control for supermagnetic and supercapacitor energy storage. Ingeniería y Ciencia 2017;13(26):147–71.

[35] Kiaei I, Lotfifard S. Tube-based model predictive control of energy storage systems for enhancing transient stability of power systems. IEEE Trans Smart Grid 2018;9(6):6438–47.

[36] Nguyen TT, Yoo HJ, Kim HM. Applying model predictive control to SMES system in microgrids for Eddy current losses reduction. IEEE Trans Appl Supercond 2016;26(4):1–5.

[37] Hou R, Song H, Nguyen T-T, Qu Y, Kim H-M. Robustness improvement of superconducting magnetic energy storage system in microgrids using an energy shaping passivity-based control strategy. Energies 2017;10(5):671.

[38] Gil-González W, Montoya OD, Garcés A, Espinosa-Pérez G. IDA-passivity-based control for superconducting magnetic energy storage with PWM-CSC. In: 2017 Ninth Annual IEEE Green Technologies Conference (GreenTech); 2017. p. 89–95.

[39] Montoya O, Gil-González W, Serra F. PBC approach for SMES devices in electric distribution networks. IEEE Trans Circuits Syst II 2018;65(12):2003–7.

[40] Ye Y, Kazerani M, Quintana VH. Current-source converter based STATCOM: modeling and control. IEEE Trans Power Deliv 2005;20(2):795–800.

[41] Fuchs FW, Kloenne A. DC link and dynamic performance features of IPEMC, 2004.

[42] Monteiro V, Pinto J, Exposto B, Afonso JL. Comprehensive comparison of a current-source and a voltage-source converter for three-phase ev fast battery chargers. In: 2015 9th International Conference on Compatibility and Power Electronics (CPE). IEEE; 2015. p. 173–8.

[43] Deben Singh M, Mehta RK, Singh AK. Integrated fuzzy-PI controlled current source converter based D-STATCOM. Cogent Eng 2016;3(1):1138921.

[44] Golestan S, Guerrero JM, Vasquez JC. Three-phase PLLs: a review of recent advances. IEEE Trans Power Electron 2017;32(3):1894–907.

[45] Pham DH, Hunter G, Li L, Zhu J. Advanced microgrid power control through grid-connected inverters. In: 2015 IEEE PES Asia-Pacific Power and Energy Engineering Conference (APPEEC); 2015. p. 1–6.

[46] Khalil H. Nonlinear systems. 3rd ed. New Jersey: Prentice-Hall; 2002.

[47] Rashid MH. Power electronics handbook-devices, circuits, and applications. Elsevier; 2011.

[48] Chapman S. Electric machinery fundamentals. Electric machinery fundamentals. McGraw-Hill Companies. Incorporated; 2005.